Journal of Non-Crystalline Solids 24 (1977) 377–398

THERMOELECTRIC POWER OF AMORPHOUS COMPOUND SEMICONDUCTORS

Hubert A. VANDER PLAS * and Richard H. BUBE

Department of Materials Science and Engineering, Stanford University, Stanford, California 94305, USA

Received 6 December 1976

Thermoelectric power measurements as a function of temperature have been made on four V-VI amorphous chalcogenides, ten IV–VI amorphous chalcogenides of the Ge_xTe_{1-x} system, and five amorphous IV–V materials. In the IV–V and the intermediate composition IV–VI materials, the charge transport cannot be described on the basis of conduction at only one energy level. The former exhibit characteristics of conduction both in extended states and in localized states at the Fermi level. Transport in the V–VI materials can be formally described in terms of conduction at one level in either the chaotic band or the small polaron models, but the use of a two-channel model with transport simultaneously in both p-type extended and localized states seems the most promising.

1. Thermoelectric power of amorphous compound semiconductors

The thermoelectric power (TEP) measurement is a useful technique in determining the transport mechanism in amorphous semiconductors. Some materials such as As_2Te_3 have been measured by a number of investigators with consistent results. The TEP and dark conductivity are each approximated by a single activation energy E_S. For sputtered films of As_2Te_3, Rockstad et al. [1], Grant et al. [2] and Moustakas and Weiser [3] all report $(E_\sigma - E_S) = 0.14$ eV. In bulk amorphous As_2Te_3, Seager et al. [4] report $(E_\sigma - E_S) = 0.17$ eV. The sign of the TEP is positive, indicating conduction by positively charged carriers. The interpretation of the experimental results in As_2Te_3 varies. Rockstad et al. [1] discuss two cases which give linear S versus $1/T$ relations; two-carrier intrinsic conduction and one-carrier conduction with a thermally activated mobility. Seager et al. [4] interpret results on the basis of the small polaron hopping model.

For the large class of amorphous materials in which the conductivity is approximated by a single activation energy over a broad temperature range, Mott [5] and others [6,7] have postulated that the Fermi energy is pinned near the middle of the band gap. The temperature dependence of the thermoelectric power S measures the

* Present address: Varian Associates, Palo Alto, California, USA.

energy difference between the Fermi energy and the energy level where charge transport occurs. In a simple one-band model with the Fermi energy pinned near the middle of the band gap, S is thermally activated with an activation energy E_S the carrier density activation energy; the difference between the conductivity and the TEP activation energies can be attributed to a mobility activation energy $E_\mu = (E_\sigma - E_S)$. If, on the other hand, conduction occurs at more than one energy level or channel within the materials, $(E_\sigma - E_S)$ may not itself be of fundamental significance, but may be simply a consequence of the ratio of the conductivities of the individual channels and the conductivity weighted sum of the TEPs of the individual channels.

If the nature of the charge transport can be determined, information can be obtained about the nature of the electronic states in which the transport occurs. A number of models for the density of states in amorphous semiconductors are based on the assumption that translational and compositional disorder causes the coordination number to vary from site to site in the material. As illustrated in fig. 1a, a density of localized states is expected to extend into the crystalline "density-of-states" gap, with density going to zero at E_A and E_B. At the energies E_V and E_C in fig. 1a, the charge transport changes from a low-mobility band-transport with a finite mobility at $T = 0$ K to a thermally activated transport between localized

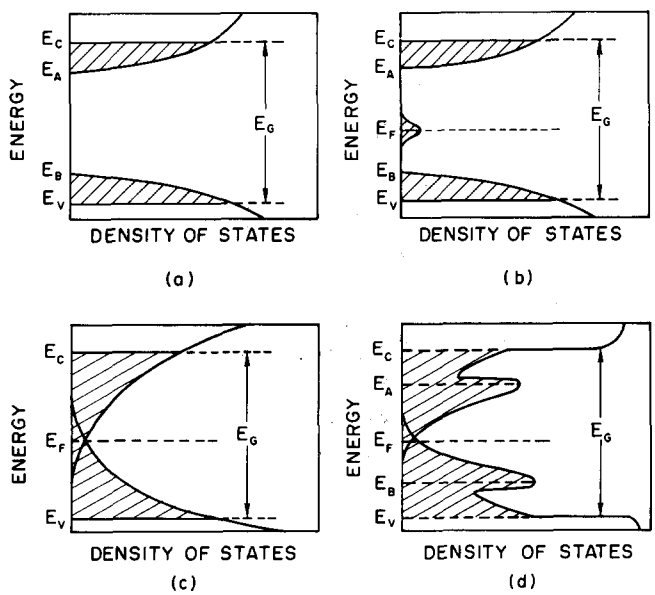

Fig. 1. Four proposed density of states models: (a) and (b) Mott and Davis [5], (c) Cohen et al. [6] and (d) Adler [7].

states that vanishes at 0 K. Energies between E_V and E_C are said to lie within the mobility gap. Mott [5] has postulated a narrow band (about 0.1 eV wide) of states pinning the Fermi level as shown in fig. 1b. Cohen et al. [6] have proposed that the density-of-states tails overlap near the middle of the mobility gap and pin the Fermi level, as shown in fig. 1c. Fig. 1d shows a modified form of fig. 1c proposed by Adler [7] after taking into account possible electronic correlation effects involving coulombic repulsive splitting of localized states. The major emphasis of this work is the interpretation of the TEP and the information the measurements provide about basic transport properties and the density of states in amorphous semiconductors.

2. Experimental

2.1. Materials

All the materials investigated in this work were prepared from their constituent elements: 6N As, 6N Sb, 5N Te, 7N Ge and 6N Sn *. Constituent elements in the desired proportions were sealed in an ampoule at 10^{-5} Torr and placed in a rocking furnace for 24 h at a temperature higher than the melting point of one or two of the constituent elements and about 100°C higher than the melting temperature of the material. Only the ternary compounds were prepared as bulk glasses. For the binary materials, immediately after quenching the material was transferred to a glove box with an oxygen-free nitrogen atmosphere, and a cathode suitable for sputtering was prepared by hotpressing. Amorphous films were prepared by sputtering in an argon atmosphere to produce 1 μm thick films on quartz **; X-ray diffraction and microprobing *** were carried out to determine the amorphous nature and the exact composition of the sputtered film. For TEP measurements, the film was deposited over a parallel gold electrode pattern previously deposited on the quartz.

2.2. Measurements

The TEP sample holder consisted of two magnesium blocks, each provided with a Zener diode operated in reverse breakdown as a heater, mounted on a copper baseplate. The sample was placed across the two heater blocks. Copper–constantan thermocouples placed on the sample measured the temperature at each end of the sample. A thin sheet of teflon between the Mg and Cu was used to minimize the

* Purchased from Electronic Space Products, Inc., Box 18795, Los Angeles, California 90018, USA.

** Sputtering was performed by William Holmes, Center of Materials Research, Stanford University.

*** Electron microprobing was performed by C. Zercher, Center for Materials Research, Stanford University.

power differential necessary to maintain a given temperature gradient. The sample holder was mounted on an Air products, Inc., Joule–Thompson expansion cooling tip.

Thermocouple voltages were recorded to the nearest microvolt, using a Keithley 171 $4\frac{1}{2}$-digit digital multimeter. The average temperature was manually controlled to remain within 0.5 K of the desired temperature. One of two electrometers was used to make the voltage measurement: a Keithley model 610B (input resistance of $10^{14}\ \Omega$) or a Ketihley model 640 vibrating capacitor electrometer (input resistance of $10^{16}\ \Omega$). Reliable measurements were made to sample resistances of $10^{10}\ \Omega$. Electrical resistance measurements were taken after each TEP plot had been recorded using the Keithley 610B electrometer in its resistance mode.

3. Theory

Theoretical expressions describing the dark conductivity and TEP vary with the energy range in which transport occurs.

(A) The conductivity due to holes excited into extended states below E_V in fig. 1b is given by

$$\sigma_1 = \sigma_{10} \exp[-(E_F - E_V)/kT] \,. \tag{1}$$

If the energy level varies linearly with temperature

$$E_f = E_F - E_V = E_f^0 - b_f T \,, \tag{2}$$

one obtains

$$\sigma_1 = C_1 \exp(-E_f^0/kT) \tag{3}$$

The TEP in the same regime is

$$S_1 = \frac{k}{e}\left[\frac{E_F - E_V}{kT} + A\right], \tag{4}$$

where A is typically calculated to be 1 for amorphous semiconductor extended state conduction [8,9].

(B) The conductivity due to holes excited into localized states, $E_V < E < E_B$ in fig. 1b, contains a thermally activated mobility and is given by

$$\sigma_2 = \sigma_{20} \exp[-(E_F - E_B + E_\mu)/kT] = C_2 \exp[-(E_b^0 + E_\mu)/kT] \,, \tag{5}$$

where $E_b = E_F - E_B = E_b^0 - b_b T$, and E_μ is the mobility activation energy. The TEP has the form

$$S_2 = \frac{k}{e}\left[\frac{E_F - E_B}{kT} + A\right], \tag{6}$$

where for hopping motion A is expected to be small and is typically taken to be zero [10].

(C) For conduction near the Fermi energy, the form of the conductivity for nearest-neighbor hopping is

$$\sigma_3 = \sigma_{30} \exp(-\Delta W/kT) , \tag{7}$$

where ΔW is a hopping activation energy. For the case of variable-range hopping, Mott [11,12] has derived the relation

$$\sigma_4 = \sigma_{40} \exp[-(T_0/T)^{1/4}] . \tag{8}$$

The form of the TEP in this regime is equivalent to metallic conduction:

$$S_3 = \frac{\pi^2}{3} \frac{k^2 T}{e} \left[\frac{1}{\sigma} \frac{\mathrm{d}\sigma}{\mathrm{d}E} \right]_{E=E_F} . \tag{9}$$

(D) If electrical conduction occurs sumultaneously at two different energy levels or channels, the measured TEP is the conductivity weighted sum of the TEPs of the individual channels:

$$S = (S_1\sigma_1 + S_2\sigma_2)/(\sigma_1 + \sigma_2) . \tag{10}$$

4. Results

The TEP and dark conductivity measurements versus temperature have been made on three categories of amorphous semiconductors: (1) V–VI materials: Sb_2Te_3, As_2Te_3, As_2SeTe_2 and As_2Se_2Te; (2) IV–VI materials: $Ge_3Se_2Te_4$ and Ge_xTe_{1-x} with x = 0.22, 0.36, 0.40, 0.47, 0.50, 0.58, 0.60, 0.68, 0.75 and 1.0 *; and (3) IV–V materials: $Sn_{55}As_{45}$, $Ge_{57}Sb_{43}$ and $Ge_{41}Sb_{59}$.

4.1. V–VI materials

The behavior of V–VI chalcogenide materials can be approximated by the following equations:

$$\sigma = C_0 \exp(-E_\sigma/kT) , \tag{11}$$

$$S = (k/e)\,[(E_S/kT) + A'] , \tag{12}$$

$$\Delta E = E_\sigma - E_S . \tag{13}$$

The temperature dependences of the TEP and dark conductivity are summarized in table 1. The temperature range of the measurements was limited at high tempera-

* Sputtering target purchased from Hazeldon Co., San Jose, California, USA.

Table 1
Transport data for V-VI materials.

Material	E_σ(eV)	E_S(eV)	ΔE(eV)	b(eV/ K) [a]	E_{op}(300 K) (eV) [b]	E_{op}(0 K) (eV) [c]
Sb_2Te_3	0.27	0.16	0.11	-4.5×10^{-4}	0.64	0.77
As_2Te_3	0.48	0.34	0.14	-4.13×10^{-4}	0.71	0.83
As_2SeTe_2	0.55	0.41	0.14	-4.55×10^{-4}	0.88	1.02
As_2Se_2Te	0.69	0.55	0.14	-5.97×10^{-4}	1.18	1.36

[a] Determined from E_{op}(300 K) and E_{op}(77 K); $E_{op}(T) = E_G^0 + bT$.
[b] Photon energy for $\alpha = 50\ cm^{-1}$.
[c] Determined from E_{op}(300 K) and b.

ture by annealing effects as the glass transition temperature was approached, and at low temperatures by high sample resistivity. The sign of the TEP indicates that the electrical transport is dominated by positively charged carriers. In all cases, the conductivity activation energy E_σ exceeds the TEP activation energy, E_S (a necessary but not sufficient criterion for a one-carrier conduction process with a thermally activated mobility). A model for electrical transport in these materials must provide a description of this measured difference between E_σ and E_S, which has a consistent value of 0.14 eV in all of the $As_2(Se_xTe_{1-x})_3$ materials.

Optical absorption measurements on these materials have been previously reported and are also shown in table 1 [13,14]. $E_{optical}$ is taken as the photon energy for an optical absorption constant of 50 cm^{-1}. Values for $E_{op}(0\ K) = E_G^0$ are obtained from linearly extrapolating measurements at 300 and 77 K to 0 K.

4.2. IV–VI materials

The properties of the Ge_xTe_{1-x} materials depend strongly on the Ge/Te ratio. The temperature dependence of the TEP and dark conductivity for these materials is shown in figs. 2 and 3 respectively, and can be approximated by relations of the form of eqs. (11) and (12). The summary given in table 2 indicates that the most Te-rich sample, $x = 0.22$, is similar to the V–VI materials, exhibiting p-type conductivity with $(E_\sigma - E_S) = 0.18$ eV. At the other extreme ($x = 0.75$ and 1.0), the materials are n-type over the entire range with an almost temperature-independent TEP. The properties of these materials with compositions at the two extremes suggest that two-carrier effects may dominate the intermediate compositions.

A minimum criterion for one-carrier conductivity is that $E_\sigma \geqslant E_S$. A second criterion is that the constant A, given in eqs. (4) or (6) and calculated from $A = A' + b_f/k$, be greater than zero. The magnitude of both the TEP and A are a third consideration. The only composition failing the first criterion is $x = 0.36$. This composition and two others, $x = 0.40$ and 0.60, fail the second criterion. Three compositions, $x = 0.47$, 0.50 and 0.58 are formally consistent with a one-carrier p-type con-

Table 2
Transport properties of Ge_xTe_{1-x} materials.

x	S(mV/ K, 300 K)	σ_0(mho/cm)	E_σ(eV)	E_S(eV)	ΔE(eV)	A'	A	b(eV/ K $\times 10^{-4}$)	E_G^0(eV)
0.22	+1.30	1.68×10^3	0.52	0.34	0.18	1.8	3.4	−5.2	1.02
0.36	+0.95	8.72×10^2	0.53	0.56	−0.03	−11.5	−7.5	−6.3	1.03
0.40	+0.90	2.45×10^3	0.58	0.49	0.09	−9.4	−6.2	−5.4	0.97
0.47	+0.95	1.08×10^3	0.45	0.31	0.14	−0.64	1.94	−5.8	0.81
0.50	+0.90	1.06×10^3	0.42	0.30	0.12	−0.86	1.21	−5.4	0.91
0.58	+0.95	6.53×10^2	0.46	0.30	0.16	−0.21	1.30	−4.5	1.04
0.60	+0.55	1.30×10^3	0.40	0.35	0.05	−6.78	−3.94	−4.94	0.95
0.67	−0.40	6.72×10^2	0.41	0.09	0.32	0.92	1.53	−4.9	0.84
0.75	−0.40	1.00×10^3	0.43	0.06	0.37	2.36	2.71	−4.94	1.01
1.00	−0.78	4.63×10^0	0.30	0.06	0.24	6.88	7.24	−4.5	0.88

$A = A' - (E_f^0/E_G^0)b/k$; $S = \pm(k/e)\ [A' + E_f^0/kT]$.

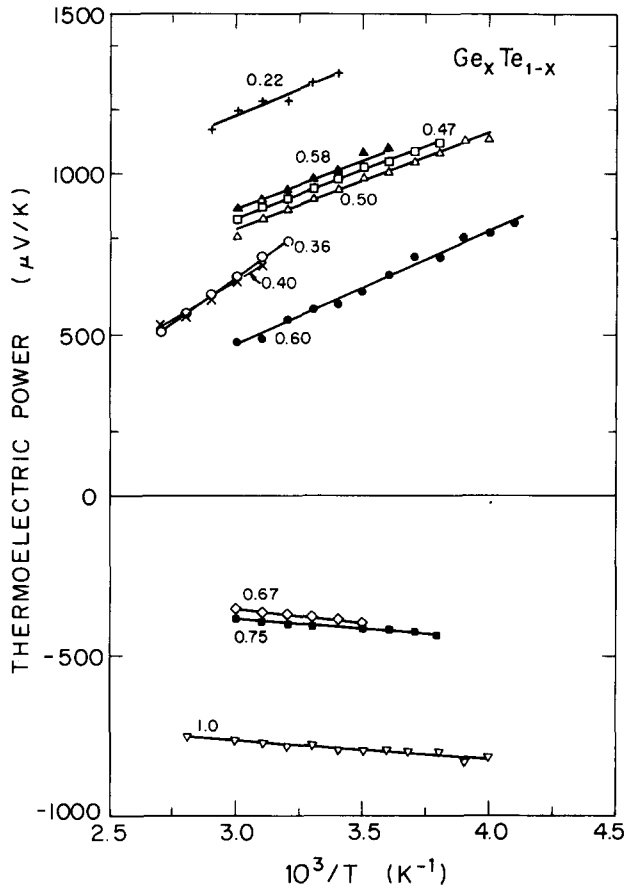

Fig. 2. Thermoelectric power as a function of reciprocal temperature for the Ge_xTe_{1-x} system.

ductivity with a thermally activated mobility. However, the value of A for these compositions is about one-half the value obtained in $Ge_{22}Te_{77}$ and As_2Te_3, and the room-temperature magnitude of the TEP is about 0.40 mV/K less than the value of $Ge_{22}Te_{77}$; both results suggest that the conductivity may have significant n-type contributions. For $x \geqslant 0.67$, the negative TEP is indicative that an n-type conduction mechanism dominates. The temperature-independent TEP may be interpreted to indicate a nearly constant carrier density with varying temperature. It is probable, however, that p-type conduction mechanisms still make a significant contribution to the conductivity in the $x = 0.67$ and 0.75 compositions since the magnitude of the TEP in these two compositions is one-half the magnitude for the $x = 1.0$ composition. In $Ge_3Se_2Te_4$, E_S (0.87 eV) exceeds E_σ (0.73 eV) and the conductivity appears to be dominated by two-carrier effects.

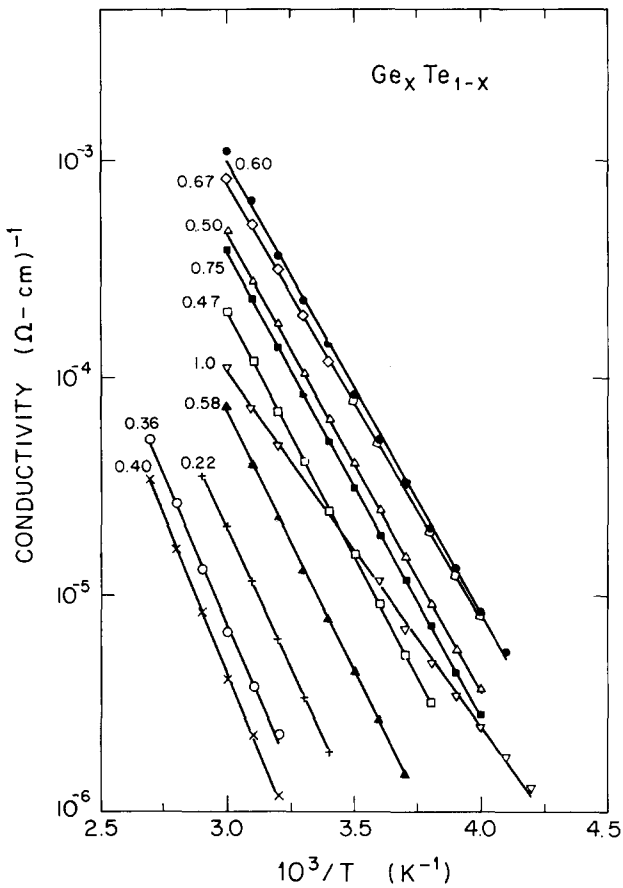

Fig. 3. Dark conductivity as a function of reciprocal temperature for the Ge_xTe_{1-x} system.

4.3. IV-V materials

Measurements on $Sn_{55}As_{45}$, $Ge_{57}Sb_{43}$ and $Ge_{41}Sb_{59}$ cannot be approximated by a single activation energy over a wide temperature range. Fig. 4 shows the data for $Sn_{55}As_{45}$. In the high-temperature range, the data can be described by eqs. (11)–(13) with $E_\sigma = 0.14$ eV, $E_S = 0.08$ eV, and $\Delta E = 0.06$ eV, consistent with one-carrier conduction with a thermally activated mobility. At low temperatures, S has decreased to a value about 0.1 of the extrapolated high-temperature behavior, indicating transport via hopping near the Fermi energy. The maximum in the $S(1/T)$ plot of fig. 4 occurs at the same temperature at which log $\sigma(1/T)$ plot deviates from the high-temperature exponential dependence.

In a material in which transport both by hopping in localized states near E_F (characterized by σ_3 and S_3) and conduction near the band edges (characterized by σ_2 and S_2) are possible, the measured TEP is given by eq. (10). At high temperatures, $\sigma_2 >> \sigma_3$, $S_2 >> S_3$ and the one-carrier model for transport near the band edge is applicable. At low temperatures, $\sigma_3 >> \sigma_2$, $S_3\sigma_3 >> S_2\sigma_2$, $S = S_3$ and the one-carrier model for transport in localized states near the Fermi level is applicable. At intermediate temperatures where $\sigma_3 > \sigma_2$, but $S_2\sigma_2 > S_3\sigma_3$, $S = (\sigma_2/\sigma_3)S_2$. These three regimes can be seen in the data of fig. 4.

The TEP and dark conductivity versus temperature for $Ge_{57}Sb_{43}$ and $Ge_{41}Sb_{59}$ are shown in fig. 5. The behavior shown here can be considered to be similar to that of $Sn_{55}As_{45}$ except that the high-temperature conduction is near the conduction-band edge rather than the valence-band edge. The hopping conduction near the Fermi energy is by holes. To confirm this hypothesis it would be desirable to measure the TEP at higher temperatures than shown in fig. 5 in order to see if pure elec-

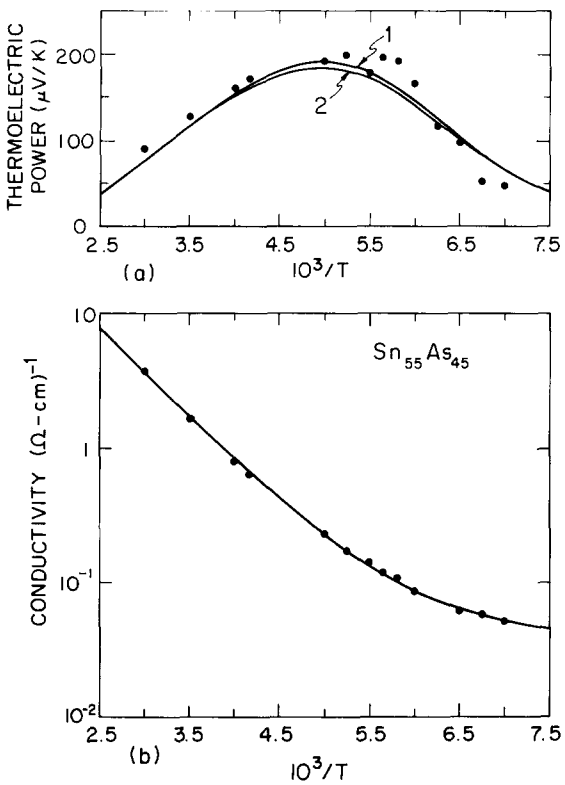

Fig. 4. Thermoelectric power and dark conductivity as a function of reciprocal temperature for $Sn_{55}As_{45}$. The lines are theoretical predictions of the thermoelectric power and dark conductivity [eqs. (14)–(17)].

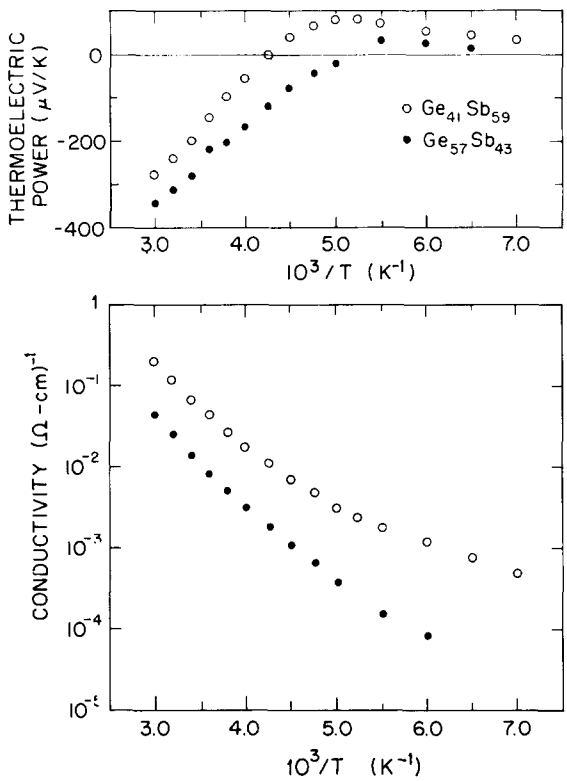

Fig. 5. Thermoelectric power and dark conductivity as a function of reciprocal temperature for $Ge_{41}Sb_{59}$ (○) and $Ge_{57}Sb_{43}$ (•).

tron conduction near the band edge could be observed; unfortunately the material crystallizes before such an observation can be made.

The measurements for all the IV–V materials are summarized in table 3.

Table 3
Transport properties of IV-V materials.

	S(300 K, μv/K)	E_σ(eV) [a]	E_S(eV) [b]	Carrier type
$Sn_{55}As_{45}$	110	0.14	0.08	p
$Ge_{57}Sb_{43}$	−300	0.12	−0.18 [c]	n, $T > 200$ K
				p, $T < 200$ K
$Ge_{41}Sb_{59}$	−230	0.22	−0.25 [c]	n, $T > 250$ K
				p, $T < 250$ K

[a] Estimated from high-temperature dependence where $\log \sigma(1/T)$ is linear.
[b] Estimated from high-temperature dependence where $S(1/T)$ is linear.
[c] Negative sign indicates that the slope is the opposite of that expected from one-carrier conduction.

5. Discussion of results

5.1. V-VI materials

A model for electrical transport in the V–VI materials must provide a description of the measured difference between the conductivity and TEP activation energies. If transport occurs at only one energy level, two basic transport models seem applicable: (1) the "chaotic band model" (CBM), and (2) the "small polaron hopping model" (SPM). A third model, the "two-channel model", assumes that electrical conduction occurs simultaneously at more than one energy level or channel.

The CBM proposed by Fritzsche [15] is illustrated in fig. 6. Since atoms in an amorphous solid are not always able to satisfy their valency requirements, the resulting "dangling bonds" and other charged defects could give rise to long-or short-range fluctuations of the energy levels within the amorphous semiconductor. If the total density of states is determined as a function of energy, the resulting density of states for the CBM is similar to the model shown in fig. 1a or 1c. For conduction by holes in the localized valleys above E_V, the dark conductivity and TEP are described by σ_2 and S_2 in eqs. (5) and (6). The mobility activation energy, $E_\mu = (E_\sigma - E_S) = 0.14$ eV in the $As_2(Se_xTe_{1-x})_3$ materials, is a reasonable estimate of the average potential barrier a charged carrier must overcome in moving from site to site.

A small polaron is defined as a unit comprised of a localized excess charge carrier and the displacement of the atomic constituents which occurs if the carrier lingers in the vicinity of an atomic site for an ample time for atomic rearrangement to occur. [4]. Assuming that hole-like polarons dominate the transport, the conduc-

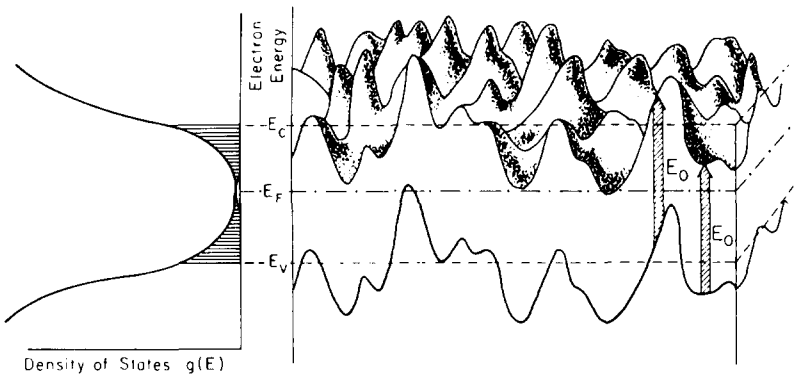

Fig. 6. Potential fluctuations of the initial and final electron states for the optical transitions corresponding to the optical gap E_G in the chaotic band model. The density of states is shown on the left-hand side (ref. [15] p. 63).

tivity and TEP take the form of σ_2 and S_2 in eqs. (5) and (6), respectively, where E_B is the polaron binding energy. The activation energy necessary for the small polaron to hop from site to site provides a physical basis for a thermally activated mobility. In As_2Te_3, Seager et al. [4] propose that a "hole-like" small polaron is associated with an As–Te bond and that conduction occurs by hopping between adjacent As–Te units. Amorphous semiconductors possessing the same dominant constituent should have similar hopping activation energies. From table 1, ΔE is equal to 0.14 eV for all of the $As_2(Se_xTe_{1-x})_3$ materials. Table 4 summarizes the TEP and conductivity for a number of investigations. Although the magnitudes of E_σ and E_S vary by as much as 0.05 eV, the difference between them is consistently 0.14 eV, the lone exception being the work of Seager et al. The consistent difference between E_σ and E_S supports the concept of a dominant constituent and conduction by small polaron hopping.

In the two-channel model proposed by Nagels et al. [10,16] conduction is proposed to be the sum of two conduction channels, one below E_V as described by σ_1 and S_1 in eq. (3) and (4) and the other in localized states near E_B described by σ_2 and S_2 in eq. (5) and (6). The measured S is described by eq. (10), while the measured conductivity is the sum of the conductivities of the individual channels. Five parameters, E_f^0, E_b^0, C_{ext}, C_{loc} and E_μ are adjusted in order to obtain a theoretical fit to both the TEP and dark conductivity data. The temperature coefficient of the extended and localized state energy levels b_f and b_b, respectively, are assumed to scale with the optical bandgap coefficient b, i.e. $b_i = (E_i^0/E_G^0)b$.

When substituted into eqs. (3)–(6) and (10), the following parameters provide the best theoretical fit to the experimental data: $E_\mu = 0.037$ eV, $E_b^0 = 0.419$ eV, $E_f^0 = 0.599$ eV, $C_1 \equiv C_{ext} = 1.1 \times 10^4$ $(\Omega\text{-cm})^{-1}$, $C_2 \equiv C_{loc} = 570$ $(\Omega\text{-cm})^{-1}$. The theoretical predictions of the measured dark conductivity and the TEP are plotted in fig. 7 and are in excellent agreement with the measured quantities over the entire range of measurements. The broken lines in fig. 7 are the theoretical conductivity and TEP plots for the individual channels. Even though the localized state conductivity dominates even at the highest temperatures measured, the contribution to the TEP from the extended states is significant over the entire measured temperature range.

The two-channel model has also been applied to the data from the bulk As_2Te_3

Table 4
Comparison of conductivity and thermoelectric power activation energies for As_2Te_3.

	E_σ(eV)	E_S(eV)	ΔE(eV)	S(300 K, μV/K)
Vander Plas and Bube	0.48	0.34	0.14	1200
Moustakas and Weiser [3]	0.44	0.30	0.14	1100
Rockstad, et al. [1]	0.43	0.29	0.14	1200
Seager et al. [4]	0.46	0.29	0.17	1200

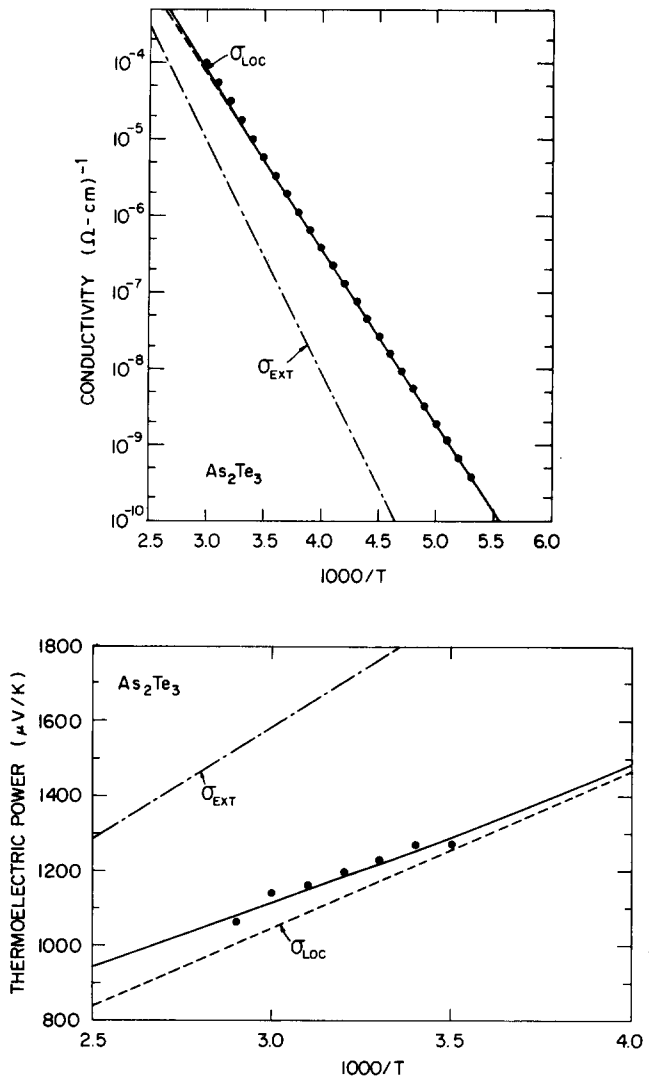

Fig. 7. Theoretical fit of the two-channel model to the thermoelectric power and dark conductivity data for sputtered As_2Te_3. The solid lines represent the total thermoelectric power and dark conductivity while the dashed lines represent the quantities for the individual channels (– – – – localized channel; —·—·— extended channel).

of Seager et al. [4]. These parameters are summarized in table 5 and compared to data for our sputtered As_2Te_3 and the bulk $AsTe_{1.5}Si_{0.025}$ of Nagels et al. [10] in both table 5 and fig. 8. It was not possible adequately to describe both the TEP and dark conductivity of the sputtered As_2Te_3 with the same parameters as those suit-

Table 5
Two-channel transport parameters

Reference	Material	C_{ext} $(\Omega\text{-cm})^{-1}$	$E_F - E_V$ (eV) ($T = 0$)	C_{loc} $(\Omega\text{-cm})^{-1}$	$E_F - E_B$ (eV) ($T = 0$)	E_μ (eV)
Vander Plas and Bube	As_2Te_3	1.1×10^4	0.599	570	0.419	0.037
Seager et al. [4]	As_2Te_3	4.2×10^3	0.467	120	0.358	0.03
Nagels et al. [10]	$AsTe_{1.5}Si_{0.025}$	3.2×10^3	0.460	90	0.353	0.03

$\sigma_{ext} = C_{ext} \exp[-(E_F - E_V)/kT]$, $\sigma_{loc} = C_{loc} \exp[-(E_F - E_B + E_\mu)/kT]$.

able for the bulk As_2Te_3, a difference that may be due to the different preparation techniques. Qualitatively, the other V–VI materials are also consistent with the two-channel model.

We conclude, therefore, that three models: the chaotic band model, the small polaron hopping model and the two-channel model, each provides a physical basis for the measured $(E_\sigma - E_S)$ and a reasonable correlation of the TEP and conductivity data. The results of other experimental techniques must be considered in order to distinguish between these models.

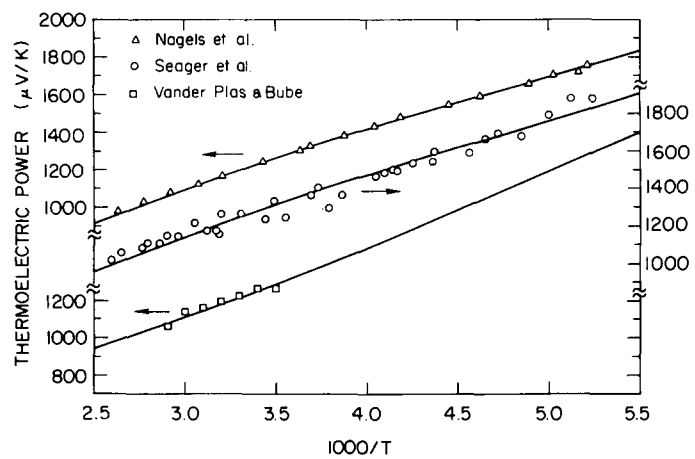

Fig. 8. Comparison of the theoretical fits of the two-channel model for sputtered As_2Te_3 (□), bulk As_2Te_3 (○), and bulk $AsTe_{1.5}Si_{0.025}$ (△). The values of the various parameters are listed in table 5.

5.2. IV-VI materials

The electrical conduction process in $Ge_{22}Te_{77}$ is similar to that in As_2Te_3. If the conductivity is a one-channel process, $E_\mu = 0.18$ eV. If it is a two-channel process, the following paramters provide the best theoretical fit to the experimental data: $E_\mu = 0.095$ eV, $E_b^0 = 0.365$ eV, $E_f^0 = 0.558$ eV, $C_{ext} = 2.50 \times 10^3$ $(\Omega\text{-cm})^{-1}$ and $C_{loc} = 80$ $(\Omega\text{-cm})^{-1}$. The theoretical predictions of the measured dark conductivity and TEP are given in fig. 9 and are in excellent agreement with the measured quantities over the entire range of measurements. The broken lines in fig. 9 are the theoretical conductivity and TEP for the individual channels. Both σ_{ext} and σ_{loc} make significant contributions to the conductivity over the entire temperature range measured.

The electrical properties of the most Ge-rich samples in the Ge_xTe_{1-x} system are distinctively different from the Te-rich samples. The TEP is almost independent of temperature from 250 to 370 K and is negative, indicating that electrons domi-

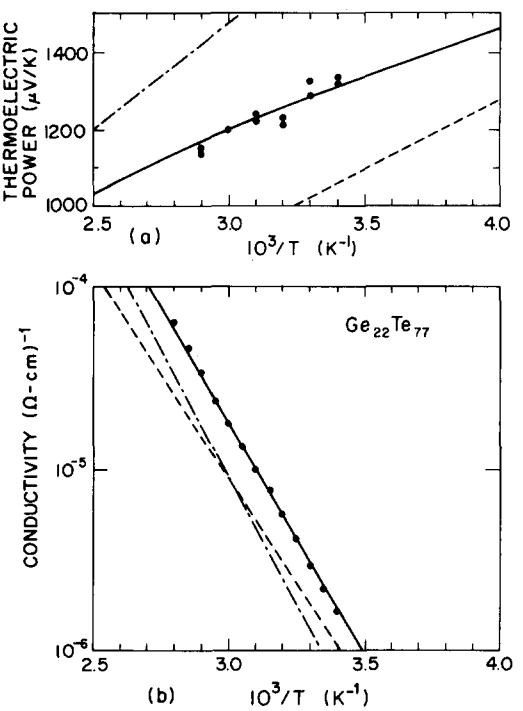

Fig. 9. Theoretical fit of the two-channel model to the thermoelectric power and dark conductivity data for $Ge_{22}Te_{77}$. The solid lines represent the total thermoelectric power and dark conductivity while the dashed lines represent the quantities for the individual channels (– – – localized channel; –·–·– extended channel).

nate the electrical transport. If this amorphous Ge (a-Ge) sample is considered to be a non-degenerate semiconductor, the TEP data indicate a high density of donor levels near the conduction-band edge. These donors are easily ionized and contribute essentially all of their electrons to the conduction band throughout the entire measured temperature range, giving an essentially constant carrier density. Recently, amorphous Si has been substitutionally doped, both n-type and p-type [1–19]. Since the amorphous Ge is deposited by vapor deposition (rf sputtering), there is a possibility of the film being doped by impurities from the residual atmosphere in the deposition chamber.

In this model, the difference between the conductivity and TEP activation energies of 0.24 eV is attributed to a "grain boundary" limited mobility. Since the films are deposited from a vapor, the growth process involves the nucleation and growth of amorphous domains. As these domains grow together, an interface region exists between domains. Donovan and Heinemann [20] (evaporated a-Ge) and Hauser and Staudinger [21] (rf sputtered a-Ge) did transmission electron microscopy on films of a-Ge up to 600 Å thick. Both teams of investigators report the existence of voids of approximately 10 Å diameter. If this void-network continued to exist in the 1 μm thick films, it could serve as a "domain boundary" network that impedes the carrier mobility; $(E_\sigma - E_S)$ could then be attributed to the activation energy necessary for the carrier to be transported across the voids. For crystalline material in which grain boundaries cause the mobility to be thermally activated, mobility activation energies as great as 0.2 and 0.3 eV have been measured [22]. Although the postulated void-network provides a possible description of the electronic behavior of a-GE, it is not possible to verify its effect on the electronic properties experimentally. It is not possible to do transmission electron microscopy on films of the thickness required to do TEP measurements.

The TEP data for $x = 0.67$ and $x = 0.75$ are very similar to a-Ge except that the room-temperature magnitude is 0.38 mV/K less than the room temperature magnitude in a-Ge. It is possible that p-type conduction mechanisms still make a significant contribution to the conductivity, accounting for the decreased magnitude compared to a-Ge.

The conduction in the intermediate compositions in the Ge_xTe_{1-x} system $(0.36 \leqslant x \leqslant 0.60)$ is a transition from the p-type conduction in $Ge_{22}Te_{77}$ to the n-type conduction for $x \geqslant 0.67$.

5.3. IV–V materials

5.3.1. $Sn_{55}As_{45}$

In a material in which transport occurs both in states near the band edges and in localized states near the Fermi level, the total conductivity is the sum of the conductivities of the individual bands and the total thermoelectric power is the conductivity weighted sum of the thermoelectric powers of the individual bands [eq. (10)]. In an initial computer model to describe the $Sn_{55}As_{45}$ data of fig. 4, trans-

port near the band edge (Characterized by σ_{be} and S_{be}) is considered to be at one energy level with a thermally activated mobility. Here, σ_{be} and S_{be} are described by eqs. (5) and (6) respectively. For transport by hopping in localized states near E_F (characterized by σ_{hop} and S_{hop}), σ_{hop} may be described by either eq. (7) for nearest-neighbor hopping or by eq. (8) for variable-range hopping; S_{hop} is described by eq. (9). The total conductivity can be fit equally well with σ_{hop} described by eqs. (7) or (8).

$$\sigma = 365 \exp\left(\frac{-0.132\ \text{eV}}{kT}\right) + \\ + 1.0 \exp\left(\frac{-0.010\ \text{eV}}{kT}\right) (\Omega\text{-cm})^{-1}\ , \tag{14}$$

$$\sigma = 365 \exp\left(\frac{-0.132\ \text{eV}}{kT}\right) + \\ + 3 \exp\left[-\left(\frac{4.5 \times 10^4\ \text{K}}{T}\right)^{1/4}\right] (\Omega\text{-cm})^{-1}\ . \tag{15}$$

As shown in fig. 4b, eqs. (14) and (15) superimpose on each other when plotted on the same graph and hence both fit the experimental data equally well. A slight difference in the theoretical thermoelectric power is apparent in fig. 4. Identical expressions are used for S_{be} and S_{hop}, i.e.

$$S_{be} = \frac{k}{e}\left[\frac{0.087\ \text{eV}}{kT} \right. \\ \left. + \left(\frac{0.087}{0.19}\right)\left(\frac{4.0 \times 10^{-4}\ \text{eV/K}}{k}\right)\right], \tag{16}$$

$$S_{hop} = \frac{\pi^2}{3}\left(\frac{k}{e}\right) kT[0.10\ \text{eV}^{-1}]\ , \tag{17}$$

where $E_\mu = 0.45$ eV, $\mathrm{d}(\ln \sigma)/\mathrm{d}E = 0.10\ \text{eV}^{-1}$, $b = 4.0 \times 10^{-4}$ eV/K and $E_G^0 = 0.19$ eV. Curve 1 is plotted using eq. (14) for the conductivity, and curve 2 is plotted using eq. (15) for the conductivity. Both curves are within experimental error of the data points. Effectively $S_{hop} \sim 0$ (taking $\mathrm{d}(\ln \sigma)/\mathrm{d}E = 0.10\ \text{eV}^{-1}$) such that $S \sim (\sigma_{be}/\sigma)S_{be}$. It is probable that σ_{be} and S_{be} are better described by the two-channel model described above, but a unique sum of three conductivites to describe the total conductivity is not obtainable and further computer modeling would not be meaningful.

5.4. Ge–Sb system

Both $Ge_{41}Sb_{59}$ and $Ge_{57}Sb_{43}$ have dominant n-type conduction at high temperatures and make a transition to p-type hopping near the Fermi level at low temperatures. The simplest model is to consider the conductivity to be the sum of a single n-type band (characterized by σ_{be} and S_{be}) and p-type hopping near E_F (characterized by σ_{hop} and S_{hop}). σ_{be} is described by eq. (5) while S_{be} is considered to have a constant value. σ_{hop} may be described by either eqs. (7) or (9), while S_{hop} is described by eq. (9). The toal conductivity of $Ge_{41}Sb_{59}$ can be fit equally well by either form of σ_{hop}.

$$\sigma = 600 \exp\left(\frac{-0.230\ \text{eV}}{kT}\right) + $$

$$+ 0.09 \exp\left(\frac{-0.065\ \text{eV}}{kT}\right) (\Omega\text{-cm})^{-1}\,, \tag{18}$$

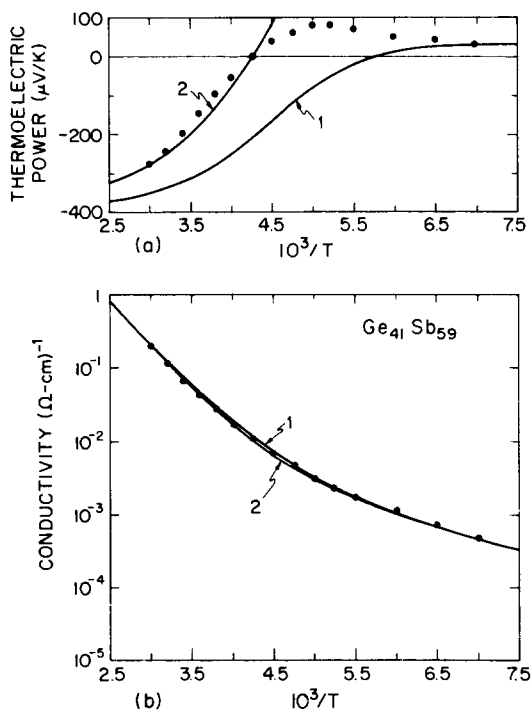

Fig. 10. Theoretical predictions of the thermoelectric power and dark conductivity fit to the data for $Ge_{41}Sb_{59}$. In (b), curve 1 is a plot of eq. (18) and curve 2 is a plot of eq. (19). In (a), curve 1 is plotted assuming $d(\ln \sigma)/dE = 10\ \text{eV}^{-1}$ and curve 2 is plotted assuming $d(\ln \sigma)/dE = 100\ \text{eV}^{-1}$.

$$\sigma = 600 \exp\left(\frac{-0.230\ \text{eV}}{kT}\right) + 3.40 \times 10^5 \exp\left[-\left(\frac{2.50 \times 10^2\ \text{K}}{T}\right)^{1/4}\right](\Omega\text{-cm})^{-1} . \quad (19)$$

Both theoretical fits are plotted in fig. 10(b) and fit the data equally well. Using eq. (10) and taking $S_{be} = -400\ \mu\text{V/K}$, S is plotted versus $1/T$ in fig. 10a for two different values of $\mathrm{d}(\ln \sigma)\mathrm{d}E$. Curve 1 for $\mathrm{d}(\ln \sigma)/\mathrm{d}E = 10\ \text{eV}^{-1}$ correctly approximates the temperature at which the measured thermoelectric power changes sign, but the low-temperature magnitude is an order of magnitude too large. Allowing S_{be} to be temperature dependent does not provide better correlation. For conduction near the band edge, the magnitude of S_{be} increases with decreasing temperature. A p-type contribution near the band edge must be postulated in order to describe the total S versus $1/T$ curve. An exact computer model requires the conductivity to be the sum of three contributions and a unique set of parameters is not obtainable. For $Ge_{57}Sb_{43}$, even the conductivity cannot be approximated by the sum of only two contributions, further supporting the need for a third contribution, probably a p-type conduction near the valence-band edge.

6. Conclusions

The TEP measurements in the V–VI materials indicate p-type conduction and are consistent with three transport models. In the chaotic band model and the small polaron hopping model, conduction is assumed to be through only one energy level or channel, and the difference between the conductivity and TEP activation energies of about 0.14 eV is atrributed to a thermally activated mobility with an activation energy $E_\mu = \Delta E = (E_\sigma - E_S)$. In the chaotic band model, the measured ΔE of 0.14 eV is a reasonable estimate of the average height of the potential fluctuations of the energy levels within the material. In the small polaron hopping model, ΔE is interpreted to be the potential barrier a charged carrier must overcome in hopping from site to site. In the third transport model – the two-channel model – conduction occurs through both p-type extended states and p-type localized states near the valence-band edge. Here ΔE is a consequence of the ratio of the conductivities and the conductivity weighted sum of the TEPs of the individual channels. Although the TEP alone cannot definitively distinguish the proper transport model, it provides necessary information that must be compared to the information from other experimental techniques in determining the proper description.

The behavior of the Ge_xTe_{1-x} materials depends on the relative proportions of Ge and Te. The most Te-rich sample ($Ge_{22}Te_{77}$) is similar to the V–VI materials and its electrical properties are consistent with the three models discussed above. a-Ge ($x = 1.0$) can be considered to be an n-type non-degenerate semiconduc-

tor with a constant electron density and a carrier mobility limited by a void-network as sometimes observed in thinner films of a-Ge. For $0.36 \leqslant x \leqslant 0.75$, two-carrier effects dominate the total conductivity.

In the IV–V materials, both n-type and p-type TEP is observed. Samples in the Ge–Sb system are n-type at high temperature and p-type at low temperature. $Sn_{55}As_{45}$ is p-type throughout the entire measurable temperature range with the low-temperature magnitude of the TEP an order of magnitude less than the high-temperature magnitude. Calculations based on the assumption of only two conduction channels (a p-type hopping in localized states near the band edge and p-type hopping in localized states near the Fermi energy) are not able to describe the complete temperature dependence of the TEP in detail. It is probable that the conduction near the band edge is best described by the the two-channel model and that the total conductivity is therefore the sum of three contributions. Similar calculations for $Ge_{41}Sb_{59}$ and $Ge_{54}Sb_{43}$, based on the assumption of only two conduction channels (an n-type channel near the band edge and a p-type hopping in localized states near the Fermi energy) seem to require an additional p-type channel near the band edge.

In the IV–V and the intermediate composition IV–VI materials, the charge transport cannot be described on the basis of conduction at only one energy level. In the V–VI materials, although the two models that propose transport at only one energy level cannot be definitively ruled out, the two-channel model gives the most promise of being able to integrate the data from a number of experimental techniques.

Acknowledgements

This research was supported by the National Science Foundation.

References

[1] H.K. Rockstad, R. Flasck and S. Iwasa, J. Non-Crystalline Solids, 8–10, (1972) 326.
[2] A.J. Grant, T.D. Moustakas, T. Penney and K. Weiser, Proc. 5th Int. Conf. on Amorphous and Liquid Semiconductors, ed. J. Stuke and W. Brenig (Taylor and Francis, London, 1974), p. 325.
[3] T.D. Moustakas and K. Weiser, Phys. Rev. B12, (1975) 2448.
[4] C.H. Seager, D. Emin and R.K. Quinn, Phys, Rev. B8 (1973) 4746.
[5] N.F. Mott and E.A. Davis, Electronic and Structural Properties of Amorphous Semiconductors, (Clarendon Press, Oxford, 1971).
[6] M.H. Cohen, H. Fritzsche and S.R. Ovshinsky, Phys. Rev. Letters, 22 (1969) 1065.
[7] D. Adler, Amorphous Semiconductors (CRC Press, Cleveland, New York–London, 1971).
[8] H. Fritzsche, Amorphous and Liquid Semiconductors, ed. J. Tauc (Plenum Press, New York–London, 1974) p. 221.
[9] M. Cutler and N.F. Mott, Phys. Rev., 181 (1969) 1336.

[10] P. Nagels, R. Callaerts, and M. Denayer, Proc. 5th Int. Conference on Amorphous and Liquid Semiconductors, ed. J. Stuke and W. Brenig (Taylor and Francis, London, 1974) p. 867.
[11] N.F. Mott, Phil. Mag. 19 (1969) 835.
[12] N.F. Mott, J. Non-Crystalline Solids, 8–10 (1972) 1.
[13] T.C. Arnoldussen, C.A. Menezes, Y. Nakagawa and R.H. Bube, Phys. Rev. B9 (1974) 3377.
[14] R.T.-S Shiah and R.H. Bube, J. Appl. Phys. 47 (1976) 2005.
[15] H. Fritzsche, J. Non-Crystalline Solids 6 (1971) 49.
[16] N.F. Mott, E.A. Davis and R.A. STreet, Phil. Mag. 32 (1975) 961.
[17] W.E. Spear, P.G. LeComber, S. Kinmond and H.H. Brodsky, Appl. Phys. Letters 28 (1976) 105.
[18] W.E. Spear and P.G. LeComber, Solid State Commun. 17 (1975) 9.
[19] J. Knights, Phil. Mag. (1976), to be published.
[20] T.M. Donovan and K. Heinemann, Phys. Rev. Letters 27 (1971) 1794.
[21] J.J. Hauser and A. Staudinger, Phys. Rev. B12 (1975) 2448.
[22] C. Wu and R.H. Bube, J. Appl. Phys. 45 (1974) 648.